

Highly Parallel Detection for MRI

Lawrence L. Wald^{1,2}; Graham Wiggins¹

¹Athinoula A. Martinos Center for Biomedical Imaging, Department of Radiology, Massachusetts General Hospital and Harvard Medical School, Boston, MA, USA

²Harvard-MIT Division of Health Sciences and Technology, Cambridge, MA, USA

Introduction

Over the past two decades, phased array detection of the MR signal has benefited from a focused and sustained engineering effort. From the introduction of the first local coils on the MAGENTOM platform in 1983, the advantages of surface coil detection could be seen. The inception of array technology in the early 1990's, where a few coils were used to extend surface coil coverage and sensitivity, clearly demonstrated the power of extending the surface coil concept with arrays. The important clinical benefit of being able to match the reception strategy to individual clinical targets was not achieved until the introduction of the Integrated Panoramic Array (IPA) on the MAGNETOM Symphony in 1997. Here, the user controls the selection of the array elements from a larger array placed on the patient. While a seemingly simple and obvious extension in flexibility, the engineering challenge of seamlessly integrating the IPA methodology is belied by its continued lack of repetition within the industry.

The final step in extending array technology came from the recognition that optimal linear combinations of the coil elements could preserve much of the sensitivity and iPAT (integrated Parallel Acquisition Technique) capability of a larger array and provide a tradeoff between signal homogeneity, sensitivity and iPAT performance. Thus, while preserving the flexibility of the IPA concept, Tim (Total imaging matrix) significantly extended performance, leading to today's state-of-the-art in array technology where the practitioner has the ability to

place over a hundred receive elements on the patient and combine them into up to 32 independent receive channels with a sophisticated mode-mixing matrix designed to optimize coverage, sensitivity and iPAT acceleration.

So, what is left to improve upon? Past success drives future development, and Tim technology has done much to fuel speculation about what the ultimate limits of array detection technology are for sensitivity and iPAT capability. In this article we examine theoretical limitations in parallel imaging technology: the so-called "ultimate SNR (signal-to-noise ratio)" and "ultimate g-factor (geometry-factor)", a measure for coil efficiency regarding its iPAT performance. Finally, we try to identify future directions for

In these "highly parallel detectors", the role of the image encoding is no less important than the role of signal detection. While we continue to think of the gradient coil as the principal "encoder" of the MR image, this view is becoming outdated. With iPAT squared (iPAT²) methodology – iPAT in 2 dimensions, acceleration rates above 10-fold can be achieved with Tim technology. Thus, the gradients account for as little as 10% of the encoding; the rest of the burden being placed on the receive array. In this scenario, the role of the MR detector array begins to more resemble the electroencephalography (EEG) or magnetoencephalography (MEG) detector. In these devices all of the spatial information is derived from the detector geometry. Although there

“While preserving the flexibility of the IPA concept, Tim significantly extended performance.”

parallel RF hardware based on the conclusion that there are still significant gains possible. In particular, we wish to explore how parallel imaging technology might benefit if the coil designer was unconstrained by the number of RF channels available on the instrument. Toward this goal, the introduction of a prototype MAGNETOM Trio, A Tim System with 128 independent receive channels has given us the opportunity to move beyond theory and try to realize the potential benefits of highly parallel array detection.

appears to be limits on the ability of the array to encode spatial information distant from the coils, the MEG/EEG case can serve to educate us on the extraction of useful spatial information when faced with an ill-conditioned inverse problem. We are only beginning to explore the potential of these methods much less the hardware needs of this unusual regime.

Basic signal and noise considerations

A principal design goal is to inductively tightly-couple the receive coil to the pre-

cessing nuclear magnetization. Because the spins in the body lie in an ionic bath (salt water), the coil is also tightly coupled to randomly fluctuating fields produced by ionic currents. The currents that happen to have frequencies within the bandwidth of the RF receiver appear as spatially uniform Gaussian distributed noise in the complex image. An equivalent picture is produced by a reciprocity argument.

Here, the effectiveness of the receive coil is proportional to its efficiency as a transmit coil. The receive noise power is proportional to the power dissipated in the conductive tissue through eddy current damping (driving the ions with the electric field associated with the changing transmit field.) In either picture, the same basic rules of thumb arise. The more effective the receive coil is at detecting the spins, the more effective it will be at receiving the noise. Thus, once “body noise dominance” has been achieved, gains in SNR can only be achieved by limiting the volume of tissue contributing the noise. For example, the coil should only interact with tissue that is of interest; tissue outside of the imaging field of view (FoV) but within the region of coil sensitivity produces only unwanted noise. Arrays take advantage of this principle by their “divide and conquer” method, where each individual array element sees only a limited “noise” region.

Three related sensitivity figures of merit for the array coil are of interest:

- a) the SNR as a function of position for un-accelerated scans,
- b) a similar SNR map for accelerated scans and
- c) the maximum acceleration achievable with an acceptable g-factor penalty. The g-factor penalty is the ratio of the unaccelerated to accelerated SNR corrected for the reduced scan time (which contributes a factor of the square root of the acceleration rate). General simulations of array coils are challenging since there are a near infinite number of design choices. Nevertheless, analyzing arrays of identical

coil elements arranged to cover simple sample geometries (such as spherical or planar regions) can provide insight into more complicated variations. One particularly illuminating approach for understanding the future benefits of larger array configurations is to analyze how the SNR is affected by a larger and larger number of array elements covering the same area [1, 2]. Studies of this kind have analyzed planar [1] and spherical arrays [2].

“The quest for higher sensitivity and improved encoding acceleration both drive exploration of the logical expansion of the array approach: increasing the number of elements and reducing the size of the receive coils.”

In the planar case [1], a square region was tiled with $N = 1, 4, 16$ and 64 square array elements in a $1 \times 1, 2 \times 2, 4 \times 4$ and 8×8 configuration. The coils were overlapped by the width of the conductor and were modeled as being 1 cm above an infinite half-space of lossy salt water ($\sigma = 0.72 \text{ S/m}$). The coils were assumed to have no inductive coupling (e.g. from perfect preamplifier decoupling or decoupling networks) but the noise correlation from their shared view of the sample noise was calculated using a full-wave analysis. The SNR was then calculated as a function of depth from the center of the array. The SNR near the array was found to scale approximately with the number of array elements per side (i.e. with \sqrt{N} where N is the total element count). Thus, a 4-fold potential sensitivity gain can be expected for tissue near the array by moving from a modest number of array elements ($N = 4$) to a “large- N ” array ($N = 64$). This gain is, however, lost for deeper tissue (depths approximately equal to the lateral size of the overall array). On the other hand, there is no depth at

which an array of fewer elements outperforms the arrays with more elements. Thus large gains near the surface are potentially achievable at the cost of an added number of receive channels and a less homogeneous sensitivity profile. The reception inhomogeneity has become increasingly less problematic with the arrival of robust normalization algorithms, such as the Normalize and Prescan Normalize features on *syngo*.

In a separate modeling study, circular coils were uniformly distributed in both a gapped and overlapped configuration around a 22 cm diameter sphere of conductive dielectric material modeling biological tissue [2]. $N = 8, 12, 16, 20, 26, 32$ and 64 circular coils were tiled on the sphere. In addition to the noise from body loading, the coils were assigned a non-body noise level determined from typical copper and preamplifier noise contributions. In addition to modeling SNR for un-accelerated scans, this work modeled the additional g-factor penalty incurred in accelerated imaging and examined the SNR as a function of B_0 and compared the model results to that expected from the so-called “ultimate” SNR; the highest achievable SNR obtainable with an arbitrarily large array whose individual sensitivity basis set satisfying Maxwell’s equations [3–5]. In the spherical case, the results were qualitatively similar to the planar case. The largest gains achieved by increasing the number of array elements (N) occurred near the coil elements. At a radius of

*Works in progress (WIP). The information about this product is preliminary. The product is under development and not commercially available in the U.S., and its future availability cannot be ensured.

9 cm in the 22 cm diameter sphere, the SNR of the unaccelerated image at 1.5T increased 3.5-fold when the number of loops was increased from 8 to 32. In this case, the dependence on N was observed to be closer to linear with N compared with the \sqrt{N} seen near the planar array. Like the planar case, however, the benefits were considerably smaller more distant from the array elements. At the center of the sphere the unaccelerated 1.5T SNR increased only ~5% with the 4-fold increase in N. At higher field strength, there was more room for improvement at the center of the object. At 7.5T for example, only a very small region in the center of the phantom was within 10% of the ultimate SNR levels for a 64-channel array [6].

Accelerated imaging showed even larger gains as coil elements were added, especially for high acceleration rates. For example at Rate = 3, the g-factor penalty was 1.4-fold larger for the 8-channel array compared to the 32-channel. At Rate = 4, this widened to a factor of 2. The final accelerated image benefits from both the intrinsic sensitivity improvements as well as the g-factor gains. An additional finding of this study was an improved SNR for the overlapping array configuration compared to the gapped configuration for the largest N coils for both unaccelerated and accelerated scans. For the smaller array, the gapped array was beneficial for accelerated scans; a result seen by other studies [7, 8].

“Ultimate” SNR of arrays

Several studies have examined the upper bound on sensitivity and spatial encoding capabilities of coil arrays. The concept of the “ultimate” SNR achievable by an RF coil was introduced by Ocali and Atalar [5]. An arbitrary coil sensitivity profile outside a sample was generated from a complete set of basis functions satisfying Maxwell’s equations (either plane waves or spherical harmonics) and a linear combination was found that maximized the SNR at a given location in the sample. This

work was expanded to include the SNR of accelerated imaging [3, 4]. The ultimate SNR for accelerated imaging is found by analyzing the performance of the complete basis set.

The first interesting conclusion of this analysis is that the sensitivity of MR detection is intrinsically limited. The significance of this for future array designs, of course, hinges on how close current array designs are to this theoretical ceiling. Comparing actual designs (such as the arrays of circular coils tiling a spherical phantom reviewed above), suggest that a 32-channel array is close to the theoretical limit at the center of the phantom [2]. Happily for the employment prospects of array designers, there is substantial room for improvement towards the periphery. At a radial location equal to 80% of the coil radius, there is still a factor of 7 to go before the theoretical limit is achieved [2].

The ultimate limitation of the ability of the array for spatial encoding (iPAT) is likely imposed by a fundamental smoothness to the coil sensitivity patterns in regions free of current sources. This fact of nature derives from Maxwell’s equations. Both studies examining the ultimate acceleration limits point out a steep drop in the SNR for accelerations above about $R = 4$ or 5 [3, 4]. For example, after this rate, the g-factor penalty was seen to rise exponentially with acceleration rate for locations near the center of the spherical sample [3]. Both studies found that moving to higher B_0 field strength postponed the rapid deterioration of SNR for rates above 4x. As with the unaccelerated SNR, the situation improves as you move closer to the array elements. Here the proximity to the wires provides more rapidly varying spatial profiles. This proximity effect allowed the 64-element array of McDougall and Wright [9] to achieve credible images with an acceleration rates of 64-fold; considerably higher than the 4 to 5-fold limit suggested by the ultimate sensitivity analysis which focused on regions far from the array.

Highly parallel arrays in practice

Historical experience with array coils quickly showed that signal detection efficiency improved with even a modest number of surface coils and that the reception uniformity and reconstruction burden could be handled with simple post-processing algorithms such as the Normalize and Prescan Normalize feature. The use of surface coils was thus able to expand into the traditional role of volume coil structures. The quest for higher sensitivity and improved encoding acceleration both drive exploration of the logical expansion of the array approach: increasing the number of elements and reducing the size of the receive coils (to cover a fixed anatomical territory). With other manufacturer’s likely to follow the Tim system’s technology, at least in channel count, 32 receive channels is becoming the new standard, and multiple groups are developing torso / cardiac [10, 11], and brain [12] [13, 14] arrays for these instruments.

Although exploring arrays of $N > 32$ channels clearly risks hitting the limits identified by the studies of the ultimate sensitivity for MR, the theory suggests there is room for improvement and such important limitations must be extensively explored experimentally. We have therefore gone on to build such arrays explicitly to determine the potential capabilities and practical limitations of even larger-N arrays (96 and 128 channels). The overall picture of these two efforts has been to support the case that parallel imaging strategies can receive expanding benefits from these “large-N” arrays.

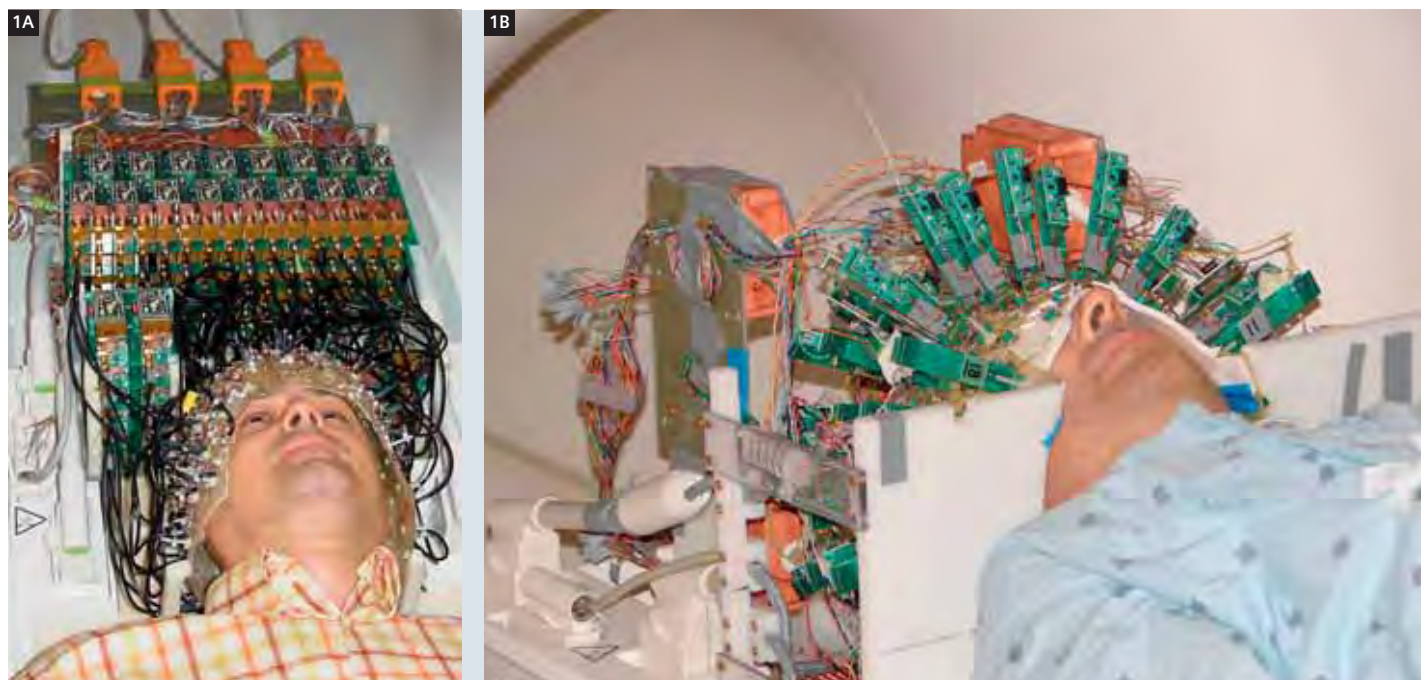
Close fitting brain arrays with 32 and 90 and 96 channels

Preliminary experience in highly parallel acquisition strategies using helmet shaped geometries of circular receive coils has concentrated on building and testing brain array prototypes for 1.5T, 3T, and 7T. Tests so far include 23 and 90-channel arrays for 1.5T [15] and 32 and 96-channel

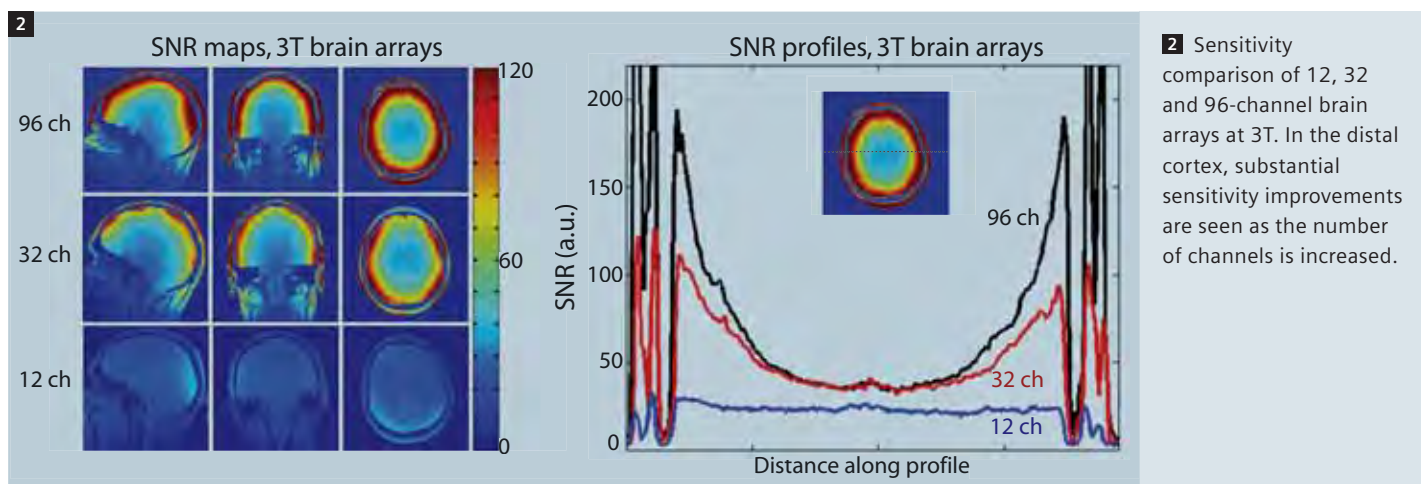
arrays for 3T [12] and 32-channel arrays for 7T. All of the arrays were built onto a helmet shaped former that conforms closely to the head. The tiling strategy for the individual circular surface coils was based on the combination of hexagonal and pentagonal symmetry of the soccer ball or the Buckminster-Fullerene molecule. Coil elements are circular, receive-only loop coils.

Figure 2 shows sensitivity maps from the 32 and 96-channel brain arrays and compares them to the standard 12-channel coil. While the 32 and 96-channel arrays are matched in size, the 12-channel coil employs a larger shell, likely exchanging the ability to accommodate a wider variety of patients with sensitivity. The larger arrays show considerable gains in the cortex with much smaller gains in the center

of the head. Nonetheless, the gains in the cortex are substantial, with nearly 10-fold increases in peripheral regions allowing the images of Figs. 3 and 4 which show brain MR images acquired with voxel volumes about 5-fold smaller than conventional acquisitions.

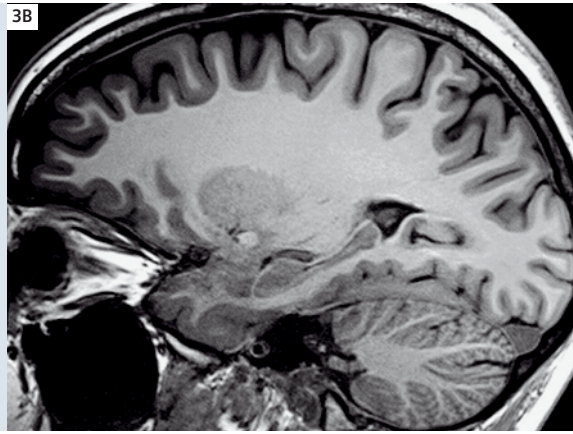
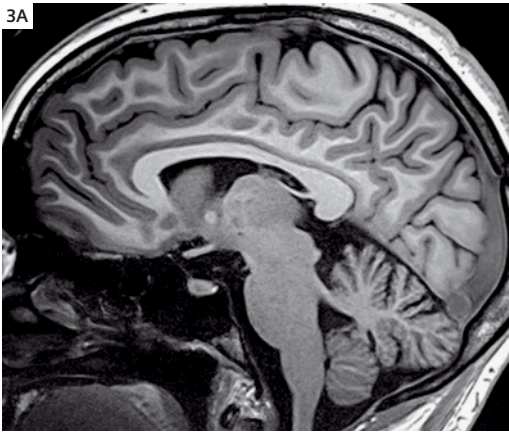


1 Graham Wiggins, one of the authors, tests the 90-channel 1.5T brain array prototype (left) and the 96-channel 3T array prototype (right). The system is a prototype 128-channel MAGNETOM Trio, A Tim System.

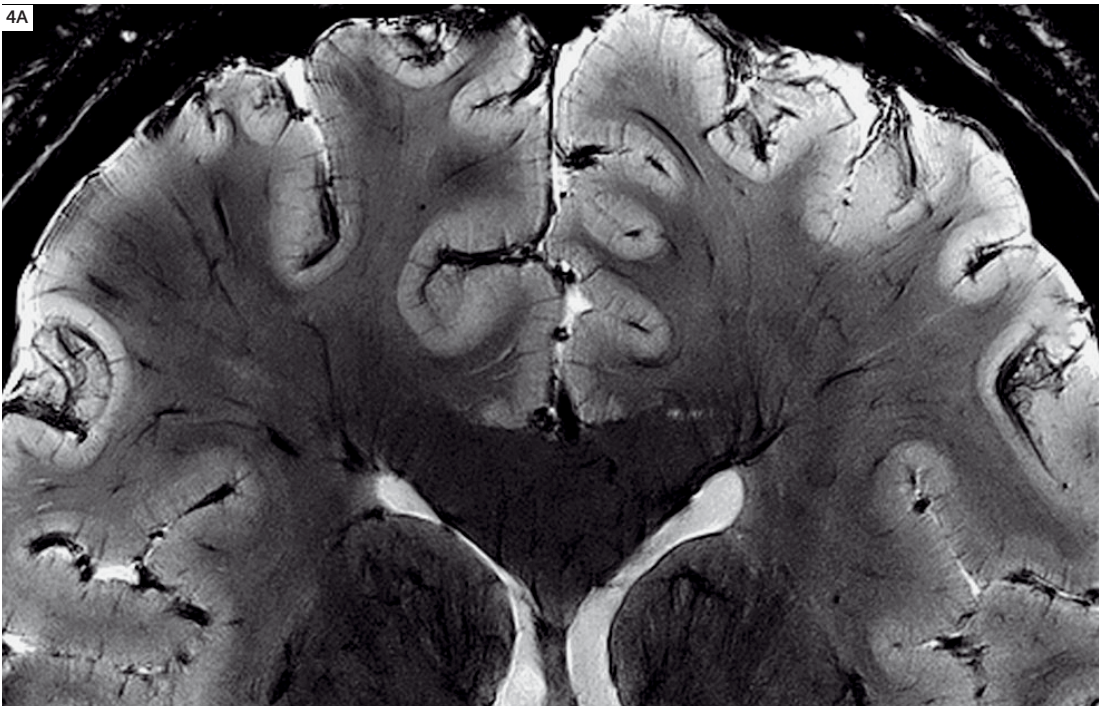


2 Sensitivity comparison of 12, 32 and 96-channel brain arrays at 3T. In the distal cortex, substantial sensitivity improvements are seen as the number of channels is increased.

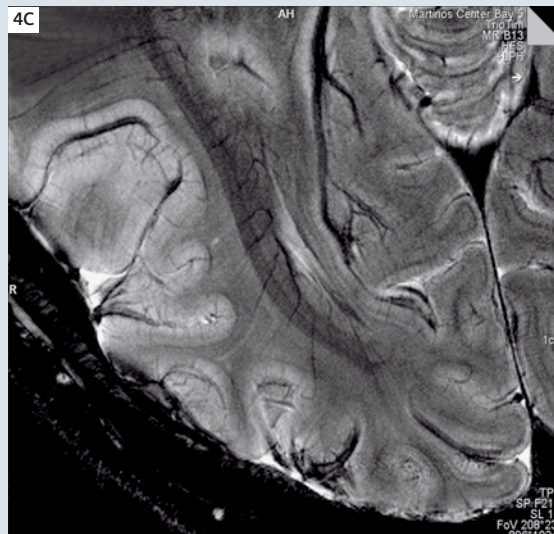
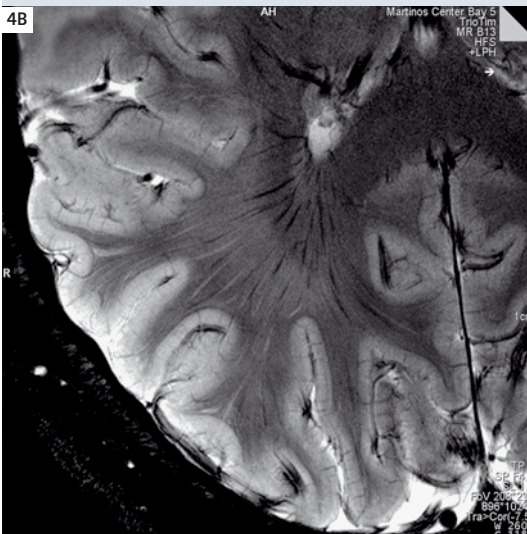
*Works in progress (WIP). The information about this product is preliminary. The product is under development and not commercially available in the U.S., and its future availability cannot be ensured.



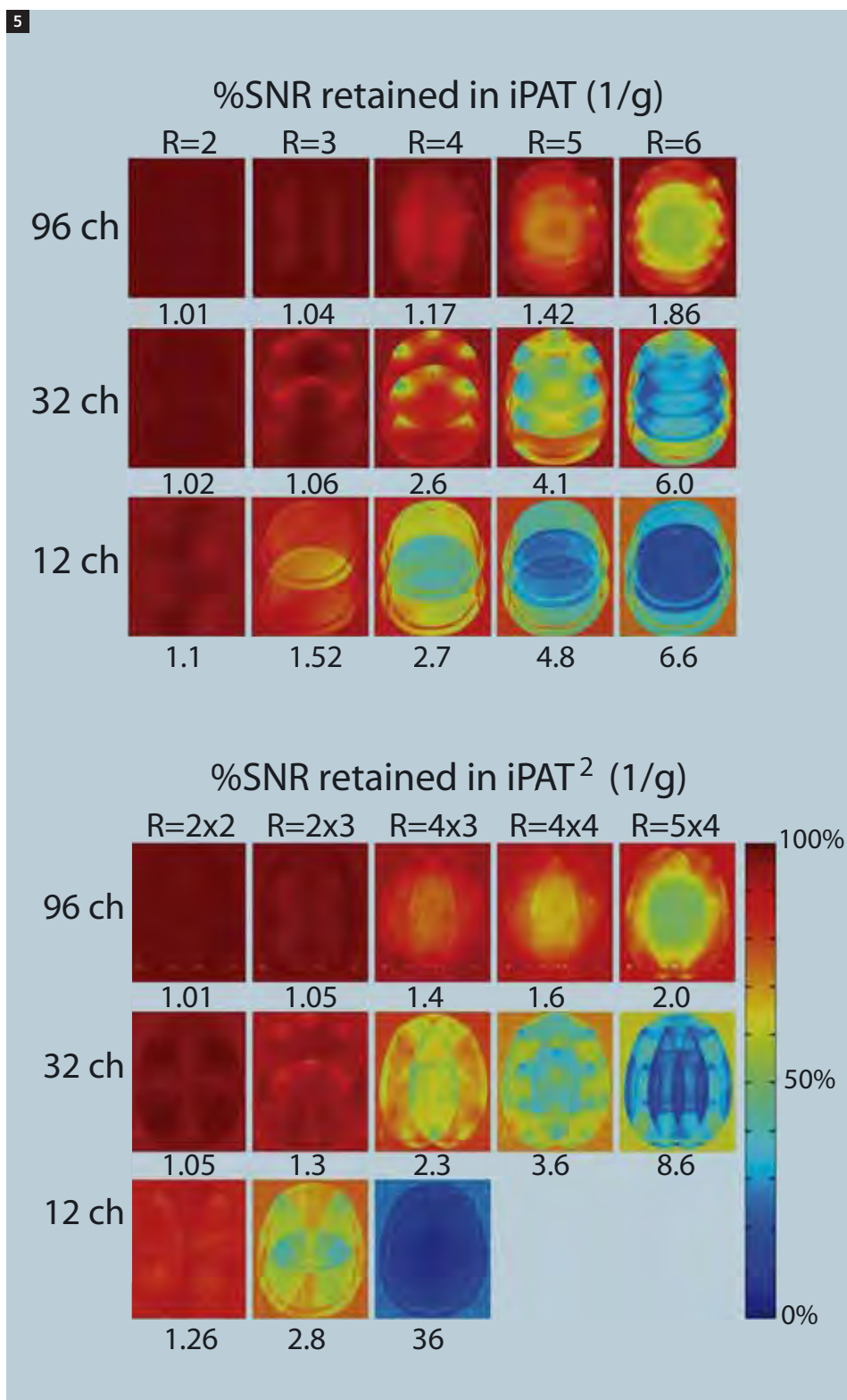
3 3 Tesla MPRAGE with a 32-channel coil (left). 500 μm in-plane resolution with a 1 mm partition thickness. 8 minutes acquisition time.



4 7 Tesla T2*-weighted imaging with a 32-channel coil. 220 μm in-plane resolution (1024 matrix) with a 1 mm slice thickness, TR/TE = 500 ms / 25 ms. 8 minutes acquisition time.



g-factor noise penalties for a given acceleration are obtained by measuring the noise correlation matrix (using a noise image acquired with no RF excitation) and coil sensitivity maps in a head shaped phantom [16]. Figure 5 shows the improved ability of the arrays for accelerated imaging. Shown is the percentage of the maximum achievable SNR, a measure related to the g-factor penalty (% SNR = 1/g) for 2 through 6-fold acceleration (conventional iPAT) as well as PAT² (acceleration in two phase encode directions) with accelerations up to 20-fold. For the higher acceleration factors, sensitivity gains up to 3-fold are seen (e.g. the R = 5 with 96 channels compared to 12 channels.) For 2-fold accelerations, extremely high accelerations (e.g. R = 4x4) are possible with the 96-channel coil. While the 32-channel coil performs significantly better with acceleration than the 12-channel coils, it still does not appear to truly push the 6x intrinsic limit identified in the ultimate g-factor calculations [3, 4]. The 96-channel array, however, appears to be close to achieving this limit.



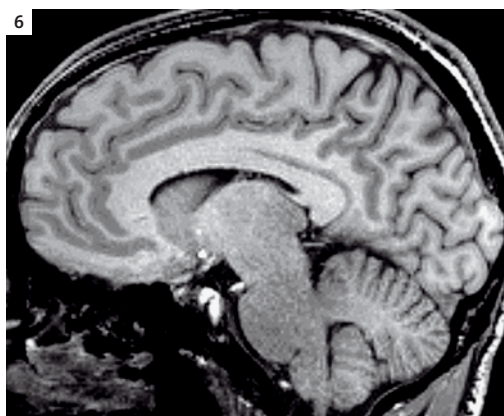
5 g-factor results for 2 thru 6x acceleration for iPAT imaging and R = 2 x 2 thru R = 5 x 4 acceleration for PAT². Maps are displayed as 1/g to allow visualization on the same scale. The maximum g-factor in the slice is given below each map. Each increase in the number of elements suggests the potential for an additional step in iPAT acceleration.

* Works in progress (WIP). The information about this product is preliminary. The product is under development and not commercially available in the U.S., and its future availability cannot be ensured.

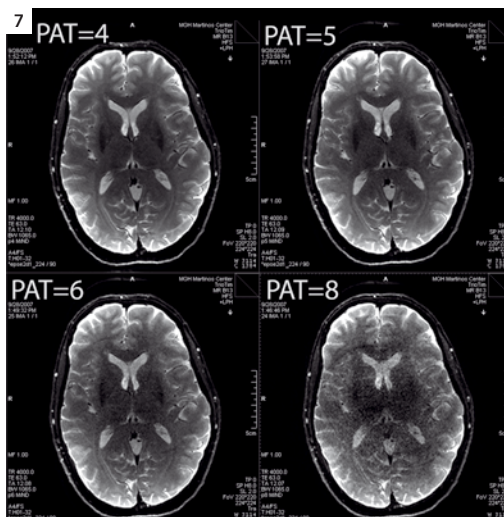
Figure 6 shows a section of a high resolution 3D FLASH image accelerated 12-fold (3x in one direction and 4x in the other) with the 32-channel 3T coil. The 1 mm spatial resolution volume acquisition was acquired in 1:20 min. Figure 7 shows spin echo EPI (echo planar imaging) acquired at millimeter resolution with single shot encoding to freeze motion. The high acceleration rates which shorten the duration of the EPI readout train help prevent geometric distortion from the susceptibility effects in the frontal lobes as well as preventing significant T2* filtering of the image during the readout.

128-channel array for cardiac MRI

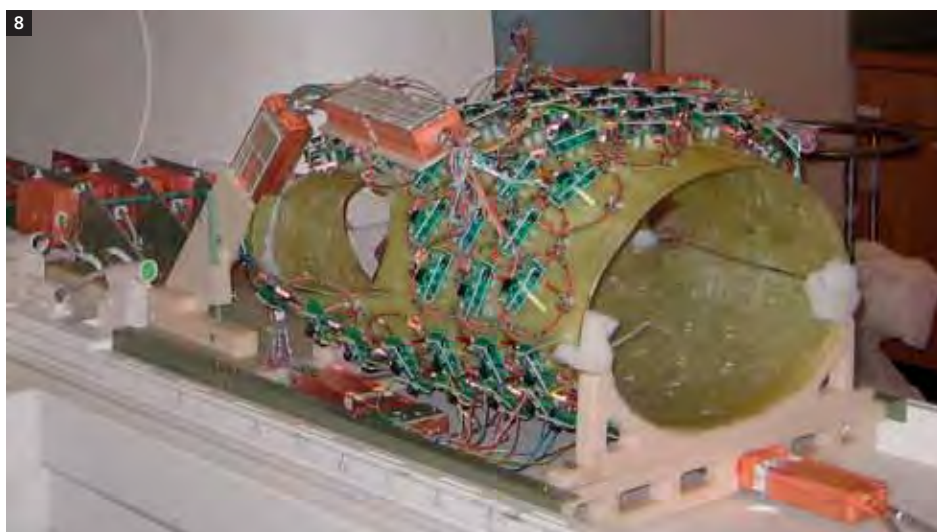
Perhaps no other application has more intrinsic need for improved accelerated imaging than 3D breathhold coronary angiograms. This motivated the extension of the “large N” array concept from brain arrays to cardiac imaging. Our prototype coil (Fig. 8) is closely contoured to the body with a “clam-shell” geometry with 68 posterior and 60 anterior elements of 75 mm diameter and arranged in a continuous overlapped array of hexagonal symmetry to minimize nearest neighbor coupling. The array was designed around accelerated imaging. For example, retaining only a subset of the elements near the heart would have likely produced similar sensitivity for non-accelerated imaging since coil elements distant from the heart contribute little to the SNR. But the accelerated image requires localized coil elements in these areas to assist with unaliasing the accelerated image.



6 A highly accelerated 3D FLASH scan acquired with the 32-channel 3T helmet array. Image was accelerated 12-fold, 4-fold in the in-plane phase encode direction and 3-fold in the thru plane phase encode direction. Image time 1:20 min, image resolution 1 mm isotropic.



7 Highly accelerated, high resolution single shot spin echo EPI acquired with the 96-channel 3T array. Tolerable artifact and noise amplification for PAT factor up to 6x. SE-EPI, 224 x 224 matrix, 220 mm, 2 mm slice thickness, TR/TE = 4 s/63 ms. Single shot encoding, with but 4 averages.



8 Prototype of a 128-channel cardiac coil. Coil is built on a fiberglass former molded to the chest shape of a 180 lbs male. The coil opens “clam-shell” style for patient access. PAT factor up to 6x. SE-EPI, 224 x 224 matrix, 220 mm, 2 mm slice thickness, TR/TE = 4 s/63 ms. Single shot encoding, with but 4 averages.

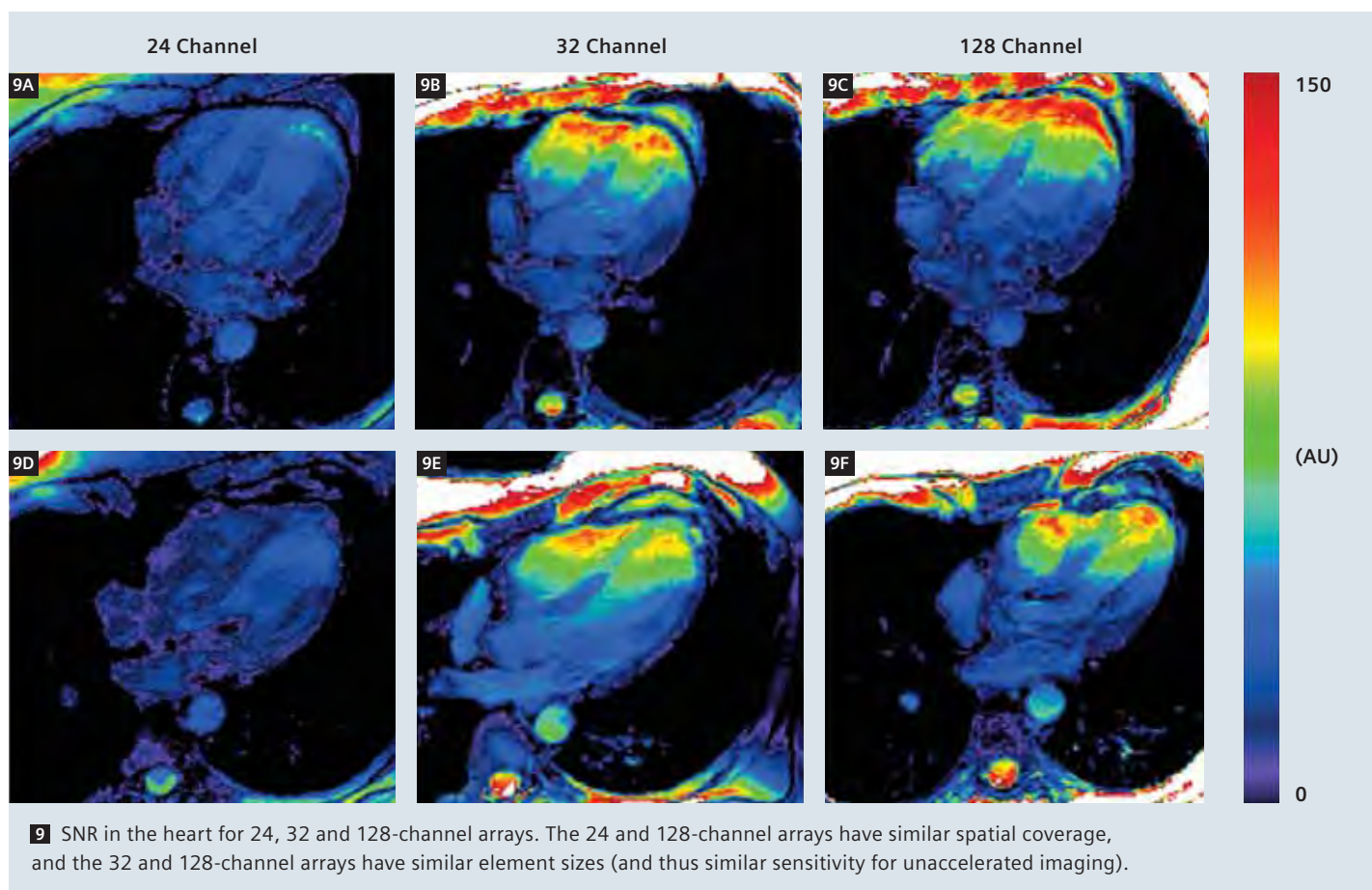
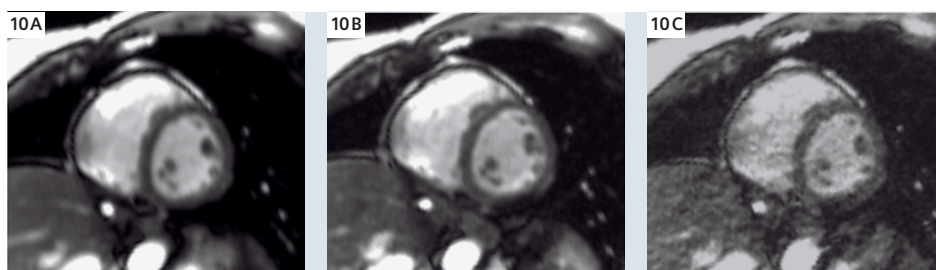
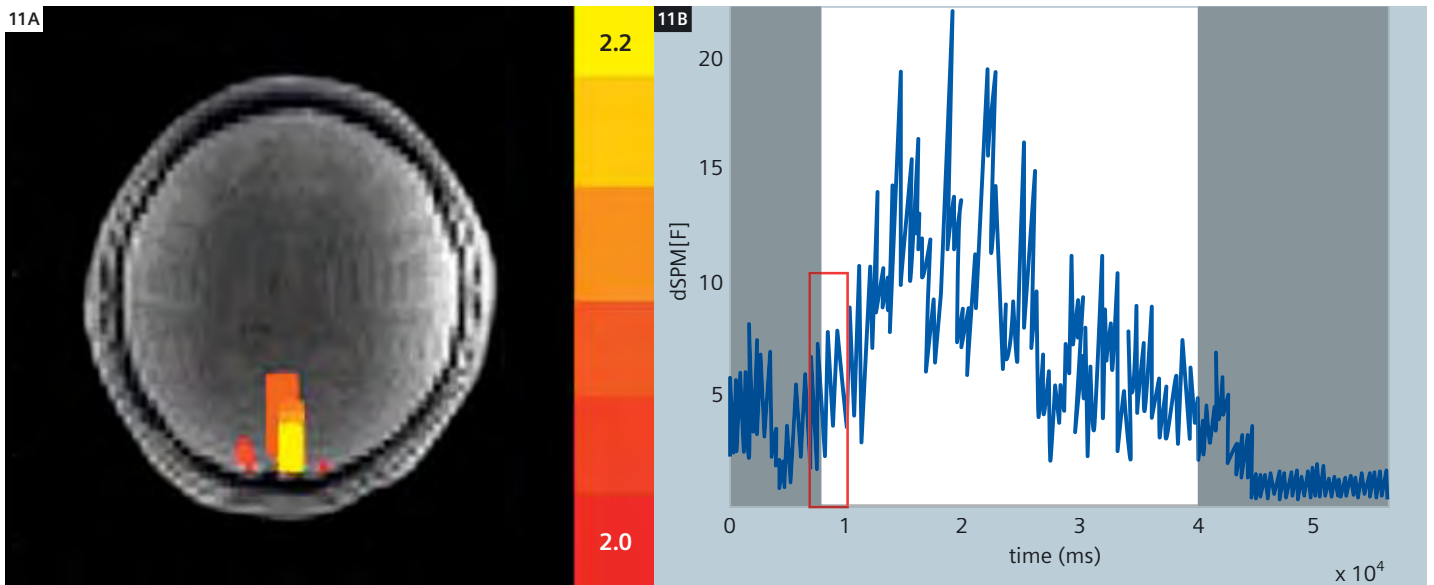


Figure 9 shows SNR maps in the heart with this coil as well as two commercial arrays. Only modest sensitivity improvements are seen relative to the 32-channel coil, which uses similar sized elements (but only covers areas near the heart.) The 128-channel coil distinguishes itself for highly accelerated imaging with maximum g-factor values at higher acceleration factors improved by a factor of 2 or more over that of the 32-channel coil. For example, at rate 5 acceleration in the head-foot direction, the maximum g-factor of the 128-channel coil reached only 1.2, and was 2.5 for the 32-channel coil. Rate 7 acceleration in the left-right direction produced a maximum g-factor value of 1.7 (128-channel array) compared to 3.4 (32-channel array).



10 High-resolution, highly accelerated 2D cine imaging performed in a female volunteer with the 128-channel cardiac coil. The SSFP cine images shown were acquired with a slice thickness of 6 mm and an in-plane resolution of 1.9 x 2.9 mm. The following acceleration factors were used: (A) rate 1, (B) rate 4, (C) rate 7. The rate 1 and rate 4 images remain almost identical (A, B), and the rate 7 images remain fully diagnostic with well-preserved blood tissue contrast and well-defined fine anatomical features.

*Works in progress (WIP). The information about this product is preliminary. The product is under development and not commercially available in the U.S., and its future availability cannot be ensured.



11 InI (MR Inverse Imaging) reconstructed statistical estimates of BOLD visual activation acquired with the 90-channel brain array. Spatial maps (left) and time series of one epoch. Temporal resolution of 20 ms was achieved with a PRESTO sequence and no phase encoding. Modulation at frequencies corresponding to the respiratory and cardiac rates are clearly visible in the time-course.

Result courtesy of FaHsuan Lin, MGH, Boston, USA.

Extreme encoding with large arrays

With current clinical systems (e.g. 32-channel), the reduction of a 10 minute volume scan to less than 1 minute with 12-fold acceleration is possible with modest increase in noise beyond the standard tradeoff between SNR and acquisition time. With even more channels (64 and 96), credible imaging can take place with truly minimal use of the gradients (for example a single readout to form an image). McDougall and Wright constructed a specialized 64-element planar array to demonstrate the potential for very high frame rate imaging acquired with no phase encode steps (e.g. all the information in this direction provided by array localization). Since the imaging is performed in a single readout, they refer to the resulting highly accelerated image as a Single Echo Acquisition (SEA) [9, 17]. Because the readout can be performed in a few milliseconds, frame rates of up to 200 fps were achievable, providing the ability to stop-motion in a paddle wheel phantom rotating at 60 rpm. In addition to illustrating the excellent image quality

(considering the 64-fold acceleration and total acquisition time of 8 ms!), their images show the potential for extreme robustness to motion.

MR Inverse Imaging (MR InI)

Using a completely different reconstruction strategy, SEA imaging was acquired in the brain using the 32 and 90-channel brain array described above. The goal was not to detect images per se, but localize the source regions of dynamic change within the brain during functional activation. In this case the goal of the MR image reconstruction resembles MEG/EEG source localization. Here, we seek statistical best estimates of the source locations and associated time courses given the spatial and temporal information available by applying the inverse solution methods used in MEG/EEG source localization. In the example shown in Fig. 8, the temporal information comes from a 50 fps PRESTO sequence acquired with no phase encoding. PRESTO was used to achieve the long TE needed for BOLD fMRI (blood oxygen level dependent functional MR imaging). The spatial information was provided by

the readout gradient (L-R direction) and the 90-channel array (A-P direction). Because of the similarity of the reconstruction to the MEG/EEG inverse problem, this approach was called MR Inverse Imaging (MR InI) [18].

Unlike conventional parallel imaging where lack of sufficient spatial information from the array manifests itself as noise amplification (g-factor), the same problem in InI produces reduced ability to spatially localize the changes; namely, a greatly reduced spatial resolution. Here, "sources" refers to the areas of the brain with dynamically altered signal with respect to user defined baseline condition. Since spatial localization is provided in one direction by the array and in the other by conventional frequency encoding, the InI method as implemented is a 1D method with slice select and standard frequency encoding providing the other spatial dimensions. It could potentially be expanded to 2D or even 3D. The 2D case is thus a Single Echo Acquisition, and the 3D case is potentially a single sample of the signal with no use of gradients. For the 90-channel array, the spatial resolution of

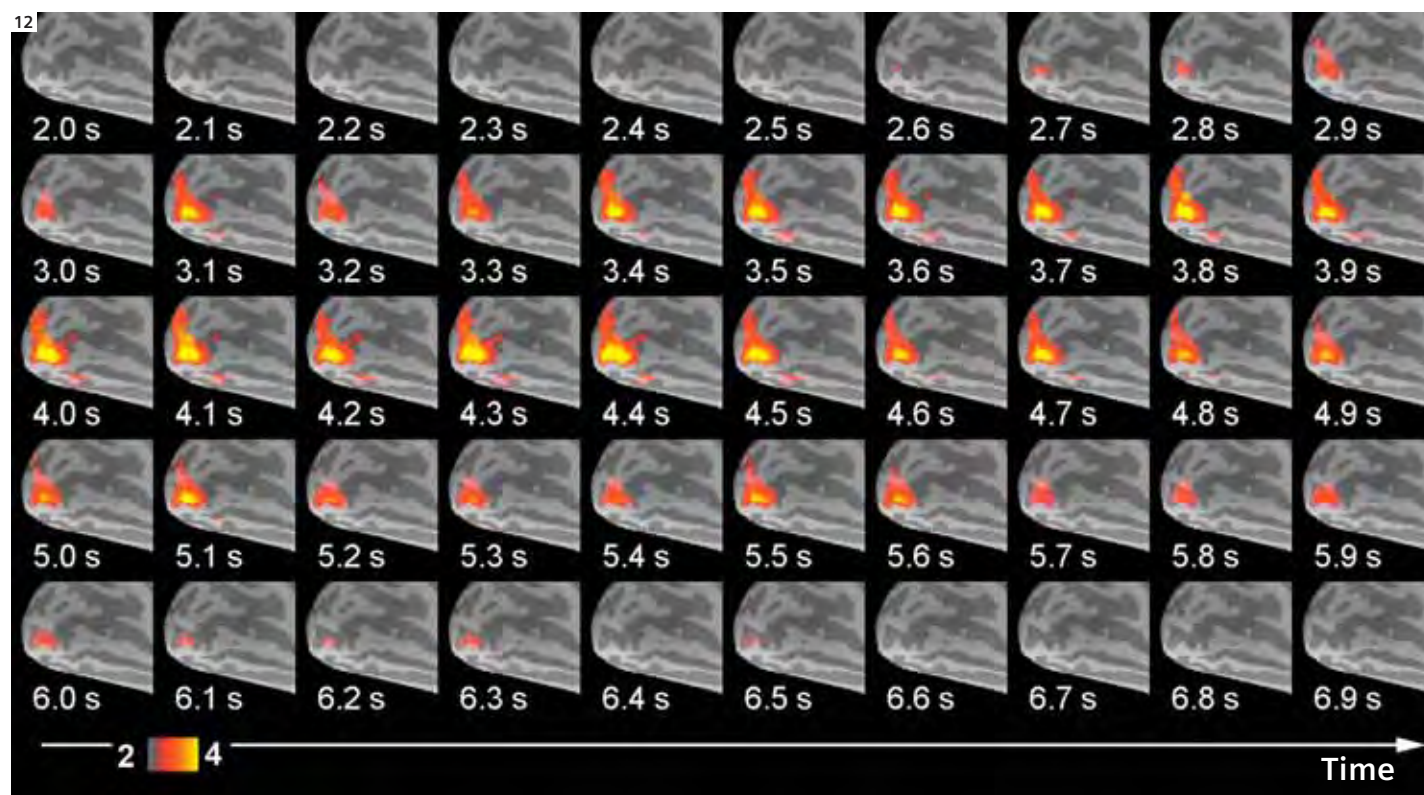
the activation localization in the 2D case was 3 mm in the readout direction and estimated to vary from just over 1 cm near the array to about 3 cm deep within the head.

Thus, in the MEG-like inverse problem, the reduced ability of the array to provide spatial information in the center of the head (where the coil profiles are too smooth to provide high spatial resolution information) translates to a deteriorated spatial resolution in these regions. Since the SNR of MR imaging scales as the cube of the voxel dimensions, a small increase in voxel dimensions may make up for reduced spatial encoding accuracy since statistical estimates will be more robust due to the higher signal levels in the

larger voxels. Thus the InI method can be viewed as coping with the encoding limitations in the center of the head by adjusting the spatial resolution accordingly. Figure 11 shows the InI reconstructed statistical estimates of the stimulus correlated changes associated with a block design visual stimulus. Also shown is the reconstructed time-course for the activated area. A temporal resolution of 50 frames per second was achieved. At this temporal resolution, many physiological modulations such as the cardiac and respiratory modulations are not temporally aliased (as they normally are) and thus potentially easily removable from the data. Figure 12 shows the extension of the InI method to 3D imaging, here the InI reconstruction is

done in the right-left direction and the other spatial directions are encoded with conventional 2D EPI. Thus, in the time it takes to acquire a conventional EPI slice (about 80 ms), the 3D InI method can do whole-head fMRI, improving temporal resolutions as much as 30-fold.

Figure 12 shows visual fMRI acquired at a whole-brain temporal resolution of 10 frames per second. The ability to significantly improve the temporal resolution of fMRI using these extreme parallel acceleration methods offers several exciting possibilities. Firstly, this will be a necessary technology for future attempts to image direct neuronal manifestations of neuronal activation (as opposed to relatively slow and more indirect hemodynamic



12 3D InI reconstructed statistical estimates of BOLD visual activation across the whole brain at 10 fps. Activation averaged across 5 subjects is shown on a representation of the inflated occipital pole.

Result courtesy of FaHsuan Lin, MGH, Boston, USA.

*Works in progress (WIP). The information about this product is preliminary. The product is under development and not commercially available in the U.S., and its future availability cannot be ensured.

effects.) MEG and EEG show these evoked responses are typically bipolar and of a duration of 30 ms or less. Thus, imaging strategies with order of magnitude improvements in the temporal resolution are needed to unambiguously resolve these events. The ability to temporally resolve significant sources of physiological modulation in the data, such as respiratory and cardiac cycle effects will also improve statistical inference in BOLD fMRI. Finally, with 3D InI there is the potential for truly silent fMRI studies of the auditory system since all gradient waveforms can be eliminated.

Conclusion

While the technical issues of building arrays with large numbers of receive elements are challenging, both the theoretical simulations and the experimental prototypes suggest the potential for substantial benefits, especially for accelerated

image encoding. The synergy between large receive arrays, higher field strength systems, and the Tim methodology also suggest that these methods will continue to evolve together in a productive way. This is seen on the theoretical side where the sensitivity gains for accelerated imaging as a function of the number of array elements were seen to improve at higher field and also on the practical side where constructing a small receive coil which is body noise dominated is easier at higher field strength.

Perhaps even more intriguing than being able to substantially improve conventional imaging, is the ability to perform new types of imaging. Realization of this potential is in its infancy but will likely have its first and largest implications for encoding-limited imaging such as high resolution 3D imaging, spectroscopic imaging, and dynamic imaging such as functional imaging.

Acknowledgements

We would like to thank Andreas Potthast, Franz Hebrank and Franz Schmitt of Siemens Medical Systems for their contribution to the large-N brain array and receiver configurations, Melanie Schmitt of MGH who developed the cardiac array, Chris Wiggins of MGH (Currently of NeuroSpin, CEA Saclay France) for his contribution to high resolution 7T studies, and FaHsuan Lin of MGH for results from the inverse imaging reconstruction method. We would like to acknowledge support from the NCCR of the NIH, grant 5P41RR014075-05, the NIH grants 1R01EB000790 and 1R01EB006847 and the MIND Institute for Mental Illness and Neuroscience Discovery.

References

- 1 Wright, S.M. and L.L. Wald, Theory and application of array coils in MR spectroscopy. *NMR Biomed*, 1997. 10(8): p. 394-410.
- 2 Wiesinger, F., N. DeZanche, and K.P. Pruessmann. Approaching Ultimate SNR with Finite Coil Arrays. in *Proceedings of the ISMRM*. 2005. Miami FL.
- 3 Wiesinger, F., P. Boesiger, and K.P. Pruessmann, Electrodynamics and ultimate SNR in parallel MR imaging. *Magn Reson Med*, 2004. 52(2): p. 376-90.
- 4 Ohliger, M.A., A.K. Grant, and D.K. Sodickson, Ultimate intrinsic signal-to-noise ratio for parallel MRI: electromagnetic field considerations. *Magn Reson Med*, 2003. 50(5): p. 1018-30.
- 5 Ocali, O. and E. Atalar, Ultimate intrinsic signal-to-noise ratio in MRI. *Magn Reson Med*, 1998. 39(3): p. 462-73.
- 6 Wiesinger, F., N. DeZanche, and K.P. Pruessmann, Approaching Ultimate SNR with Finite Coil Arrays, in *ISMRM 13th Annual Scientific Meeting*, presentation 672. 2005: Miami FL.
- 7 Weiger, M., et al., Specific coil design for SENSE: a six-element cardiac array. *Magn Reson Med*, 2001. 45(3): p. 495-504.
- 8 de Zwart, J.A., et al., Design of a SENSE-optimized high-sensitivity MRI receive coil for brain imaging. *Magn Reson Med*, 2002. 47(6): p. 1218-27.
- 9 McDougall, M.P. and S.M. Wright, 64-channel array coil for single echo acquisition magnetic resonance imaging. *Magn Reson Med*, 2005. 54(2): p. 386-92.
- 10 Zhu, Y., et al., Highly parallel volumetric imaging with a 32-element RF coil array. *Magn Reson Med*, 2004. 52(4): p. 869-77.
- 11 Sodickson, D.K., et al., Rapid volumetric MRI using parallel imaging with order-of-magnitude accelerations and a 32-element RF coil array: feasibility and implications. *Acad Radiol*, 2005. 12(5): p. 626-35.
- 12 Wiggins, G., et al. A 32 Channel Receive-only Phased Array Head Coil for 3T with Novel Geodesic Tiling Geometry. in *Proceed. International Soc. of Magnetic Resonance in Medicine*. 2005. Miami FL.
- 13 Moeller, S., et al. Parallel Imaging Performance for Densely Spaced Coils in Phase Arrays at Ultra High Field Strength in *Proceed of the 12th Annual ISMRM meeting*. 2004. Kyoto Japan.
- 14 Cline, H., et al. 32 channel head array for highly accelerated parallel imaging. in *Proceedings of the 12th annual meeting of ISMRM*. 2004. Kyoto Japan.
- 15 Wiggins, G., et al. A 96-channel MRI System with 23- and 90-channel Phase Array Head Coils at 1.5 Tesla. in *Proceed. International Soc. of Magnetic Resonance in Medicine*. 2005. Miami FL.
- 16 Pruessmann, K.P., et al., SENSE: sensitivity encoding for fast MRI. *Magn Reson Med*, 1999. 42(5): p. 952-62.
- 17 McDougall, M.P. and S.M. Wright, Phase compensation in single echo acquisition imaging. Phase effects of voxel-sized coils in planar and cylindrical arrays. *IEEE Eng Med Biol Mag*, 2005. 24(6): p. 17-22.
- 18 Lin, F.H., et al., Dynamic magnetic resonance inverse imaging of human brain function. *Magn Reson Med*, 2006. submitted.